



Ambient light-based optical biosensing platform with smartphone-embedded illumination sensor



Yoo Min Park, Yong Duk Han, Hyeong Jin Chun, Hyun C. Yoon*

Department of Molecular Science and Technology, Ajou University, Suwon, 443749 South Korea

ARTICLE INFO

Article history:

Received 17 June 2016

Received in revised form

15 August 2016

Accepted 1 September 2016

Available online 2 September 2016

Keywords:

Illumination sensor

Smartphone-based biosensor

Ambient light condition

Osteoarthritis

ABSTRACT

We present a hand-held optical biosensing system utilizing a smartphone-embedded illumination sensor that is integrated with immunoblotting assay method. The smartphone-embedded illumination sensor is regarded as an alternative optical receiver that can replace the conventional optical analysis apparatus because the illumination sensor can respond to the ambient light in a wide range of wavelengths, including visible and infrared. To demonstrate the biosensing applicability of our system employing the enzyme-mediated immunoblotting and accompanying light interference, various types of ambient light conditions including outdoor sunlight and indoor fluorescent were tested. For the immunoblotting assay, the biosensing channel generating insoluble precipitates as an end product of the enzymatic reaction is fabricated and mounted on the illumination sensor of the smartphone. The intensity of penetrating light arrives on the illumination sensor is inversely proportional to the amount of precipitates produced in the channel, and these changes are immediately analyzed and quantified via smartphone software. In this study, urinary C-terminal telopeptide fragment of type II collagen (uCTX-II), a biomarker of osteoarthritis diagnosis, was tested as a model analyte. The developed smartphone-based sensing system efficiently measured uCTX-II in the 0–5 ng/mL concentration range with a high sensitivity and accuracy under various light conditions. These assay results show that the illumination sensor-based optical biosensor is suitable for point-of-care testing (POCT).

© 2016 Elsevier B.V. All rights reserved.

1. Introduction

The development of a rapid, accurate, and sensitive diagnostic device for point-of-care testing (POCT) is a major goal for those in clinical and commercial medical fields. Recently, new biosensing techniques have improved the reliability of POCT devices by reducing operation time. Diagnostic testing is a fundamental part of a medical practice. Because the time needed for diagnostic tests has been shortened and the digitized results are integrated with the medical records, a doctor can receive patient information in a rapid and efficient manner, thus increasing the efficiency of patient care (Uys et al., 2009).

Although high-end biosensor technologies provide reliable diagnostic test results, most analyses are performed at the clinical and laboratory levels. In general, diagnostic equipment is expensive and needs a high-voltage power supply and skilled technicians to maintain it. In addition, the complexity of most high-end technologies makes them inaccessible to patients (Mabey et al., 2004; Peeling and Mabey, 2010). Many researchers have

tried to develop a novel diagnostic device for practical use by using a smart information technology (IT) device for diagnostic tests at the point of care (Martinez et al., 2008). The features of the latest-generation smartphones, such as a charge-coupled device (CCD) camera, multicore processor, touch screen, well-organized display, high computing capability, ability to take high-resolution images, and an open-source operating system, meet the needs of a diagnostic test device. These high-quality characteristics make the success of a simple and powerful biosensor integrated into a smartphone possible. The versatility of the smartphone in the biosensing system allows for alternative data analyses, display of the results on the screen, and a biosensing operation button originally used in readout devices. This approach allows the simplification of the principal design, minimization of the sample size, and reduction of the cost of the biosensor, all of which enable the production of a portable POCT device. Therefore, the smartphone with an integrated biosensor is a promising tool for obtaining practical healthcare diagnoses. In addition, smartphone ownership has increased tremendously, so a user-centered biosensor that is easy to use and inexpensive is possible. Optical and electrochemical biosensors integrated into a smartphone could detect micro- or nanoscale biocomponents such as viruses, DNA, and proteins (Breslauer et al., 2009; Bhandodkar and Wang, 2014; Chun

* Corresponding author.

E-mail address: hcyoon@ajou.ac.kr (H.C. Yoon).

et al., 2014; O'Driscoll et al., 2013; Pablos et al., 2014; Roda et al., 2014; Salles et al., 2014). Although this approach validated the high reliability and feasibility of our sensor as a diagnostic tool, it still required an additional device to provide specific functionality to the smartphone, which decreased its usability and portability. To overcome the limitation, we attempted to simplify the complex optical sensing system by producing a simple electronic component to be installed in a smart IT device. The brightness of the display of current smartphones immediately changes with the intensity of the external light because the illumination sensor embedded in the smartphone responds to the integrated light intensity of a wide range of wavelengths. This makes it possible to use various types of light, including monochromatic and polychromatic light, as the light source. Thus, ambient light such as sunlight and indoor lighting could be used as a natural light source, which would allow the use of the smartphone with the embedded biosensing chip for practical diagnosis anywhere without additional equipment. In our previous study, we successfully validated the feasibility of a light-emitting diode (LED)-based illumination biosensor, but a light-tight condition and a specific light source were needed, thus limiting its operation as well as high complexity (Park et al., 2015a). However, the present study shows that the ambient light-based biosensor can be utilized without any light source restrictions.

To make the smartphone-embedded illumination sensor an optical signal transducer in a biosensing system, we had to apply the principle of the biochemical immunoblotting assay, in which the intensity of light decreases over a wide wavelength range, to the optical sensing system to be used in ambient light such as sunlight and indoor light [Fig. 1(A)]. The insoluble precipitate produced by the immunoblotting assay reaction reduces the penetration of a broad spectrum of ambient light; hence, the light intensity changes with the target analyte concentration. The target analyte can be quantitatively analyzed by determining the change in light intensity using the lux meter application on the smartphone [Fig. 1(B)].

As an analyte, we selected the urinary C-terminal telopeptide fragment of type II collagen (uCTX-II), an osteoarthritis (OA) biomarker (Elsaid and Chichester, 2006; Garnero et al., 2005; Reijman et al., 2004). Because the structure of uCTX-II has a monomeric epitope or a variant of it (EKGDP), a smartphone-based competitive immunoassay of uCTX was conducted (Eyre et al., 2008; Kong et al., 2006) as follows: the competitive molecule PEG₄-EKGDP was immobilized on the surface of the biosensing channel

using the polydopamine modification technique (Han et al., 2014; Lee et al., 2007; Park et al., 2015b). The prepared uCTX-II samples were premixed with horseradish peroxidase (HRP)-conjugated uCTX-II antibody and then loaded onto the biosensing channel. After completion of the uCTX-II competition assay, the biosensing channel was placed on the illumination sensor upon which sunlight and indoor lighting were applied. The change in light intensity was immediately displayed numerically on the smartphone screen, allowing the quantification of the uCTX-II via the smartphone-based biosensing platform. The details of the biosensing system and its analytical performance are reported herein.

2. Experimental section

2.1. Materials

The Sylgard[®] 184 silicone elastomer kit was obtained from Dow Corning (Auburn, MI, USA), dopamine hydrochloride was purchased from Sigma-Aldrich (St. Louis, MO, USA), 3,3'-dithiobis (sulfosuccinimidyl propionate) (DTSSP) was obtained from Pierce (a part of Thermo Fisher Scientific, Waltham, MA, USA), and peptide fragments EKGDP and PEG₄-EKGDP were provided by Peptron Inc. (Daejeon, South Korea). 3,3',5,5'-Tetramethylbenzidine membrane (TMBM) substrate solution was purchased from Sur-Modics (Eden Prairie, MN, USA) and the uCTX-II ELISA kit containing an HRP-labeled monoclonal anti-uCTX-II antibody was obtained from Immunodiagnostic Systems Inc. (Tyne & Wear, UK). Double-distilled and deionized water (DDW) with a specific resistance greater than 18 MΩ cm was used for the solutions in all experiments.

2.2. Fabrication and surface modification of the reaction channel

The biosensing channel was made of polydimethylsiloxane (PDMS) and one-sided adhesive polyethylene terephthalate (PET) film. The mold used to cast the PDMS was composed of acrylic resin. To fabricate the biosensing channel, the PDMS monomer and its initiator (at a volume ratio of 10:1) were poured onto the acrylic resin mold and placed in a vacuum oven at 80 °C for 60 min. The solidified PDMS substrate was then separated from the mold and washed with DDW. The fabricated PDMS channel contained one inlet hole and one outlet hole (20 mm long × 5 mm wide × 2 mm deep) and had a volume of 200 μL. A polydopamine coating

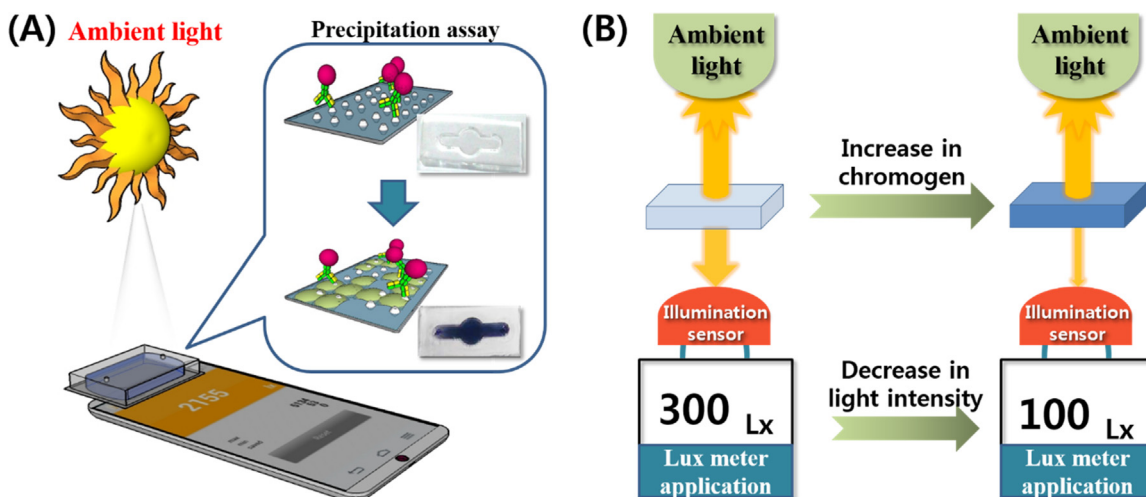


Fig. 1. Schematic illustration of the smartphone-based illumination sensor. (A) Configuration of the illumination sensor with ambient light as the light source; the biosensing channel containing precipitate is located on the illumination sensor. (B) Signaling principle of the optical biosensing system.

method was used to construct the biorecognition layer in the biosensing channel. Dopamine hydrochloride (2 mg/mL) was dissolved in 10 mM Tris-HCl buffer solution (pH 8.5) and the dopamine solution was injected into the prepared channel and kept at room temperature under darkroom conditions for 16 h. The polydopamine-coated reaction channels were then washed and filled with DDW.

2.3. Fabrication of biosensing layer for uCTX-II competition immunoassay

To fabricate the biosensing layer for the competitive uCTX-II immunoassay, we used the self-assembled monolayer technique with peptide immobilization. First, 5 mM of DTSSP solution in phosphate-buffered saline (PBS) was injected into the polydopamine-coated sensing channel and incubated for 3 h. After washing, PEG₄-EKGPDP peptide (20 µg/mL) was loaded into the channel and left for 1 h to yield the covalent immobilization of PEG₄-EKGPDP on the channel surface via amide bond formation. In this study, EKGPDP hexapeptide was used as a target analyte because the EKGPDP sequence is the epitope of uCTX-II. Furthermore, 20 mM of ethanolamine and 0.1% bovine serum albumin (BSA) were injected into the channel over 30 min to block the functional group of polydopamine that did not undergo reaction and DTSSP, respectively. Different concentrations of uCTX-II (0–5 ng/mL) were prepared and applied to the fabricated biosensor. The samples were mixed with the HRP-conjugated anti-uCTX-II antibody at a 1:3 volumetric ratio for 1 h. The mixed solutions were injected into the peptide-modified biosensing channel and incubated for 30 min. After washing, TMBM reagent was loaded into the channel and then the color-developed channel was placed on the illumination sensor in the smartphone. Furthermore, changes in the light intensity with respect to the uCTX-II concentrations were compared and registered via the lux meter application.

3. Results and discussion

3.1. Reactivity test of smartphone-embedded illumination sensor to various light wavelengths

In our previous study, we validated the illumination sensor-based optical biosensing system using the smartphone-embedded white LED as the light source. However, to use the biosensing

system indoors or outdoors, it must be used with different light sources, so we designed a new illumination sensor for ambient light such as fluorescent light and sunlight. To confirm the reactivity of the smartphone-embedded illumination sensor to light of different wavelengths, we selected the three primary colors red, green, and blue. Each of the 450-, 532-, and 635-nm monochromatic lasers used for those colors was fixed above the illumination sensor of the smartphone via plastic scaffolding [Fig. 2(A)].

The lux meter application measured the light intensity from each laser under dark conditions to prevent interference by external light. Light intensities of 5500, 6150, and 2150 lx were registered for the 450-, 530-, and 635-nm lasers, respectively, indicating that the illumination sensor responded to the applied laser sources [Fig. 2(B)]. Although the test validated the reactivity of the illumination sensor, the detected lux values were different, probably because of the difference in laser specifications. The results show that the illumination sensor responded to a wide wavelength range. In general, the illumination sensor installed in a smartphone is a silicon PIN-type photodiode, which usually receives light in the 400–1100-nm wavelength range, as indicated in the product specifications. Thus, the results obtained were reliable. On the basis of the acquired results, we verified the reactivity of the illumination sensor for various light sources and different ambient light applied to the biosensing system.

3.2. uCTX-II analysis using indoor lighting

To use the biosensing system in practical situations, we designed the ambient light-based biosensing platform. First, we used fluorescent light as the light source so the biosensing system could be used indoors [Fig. 3(A)].

The illumination sensor and the lux meter application on an LG G3 (LG-F460L) smartphone were used to measure the intensity of the fluorescent light. The measured lux value of 315 lx, shown in Fig. 3(B), was used as a background signal. To verify the reproducibility of the background signal, the same test was repeated at least three times, and the standard deviation was calculated as approximately 5%, which indicated that the illumination sensor had a stable response to the fluorescent light. On the basis of this result, we applied different concentrations of uCTX-II, from 0 to 1.2 ng/mL and prepared in buffer solution, to the illumination sensor and used indoor fluorescent lighting as the light source. Fig. 3(C) shows that the lux value gradually changed with the different uCTX-II concentrations, indicating that the insoluble precipitate in the biosensing channel, induced by immunoblot

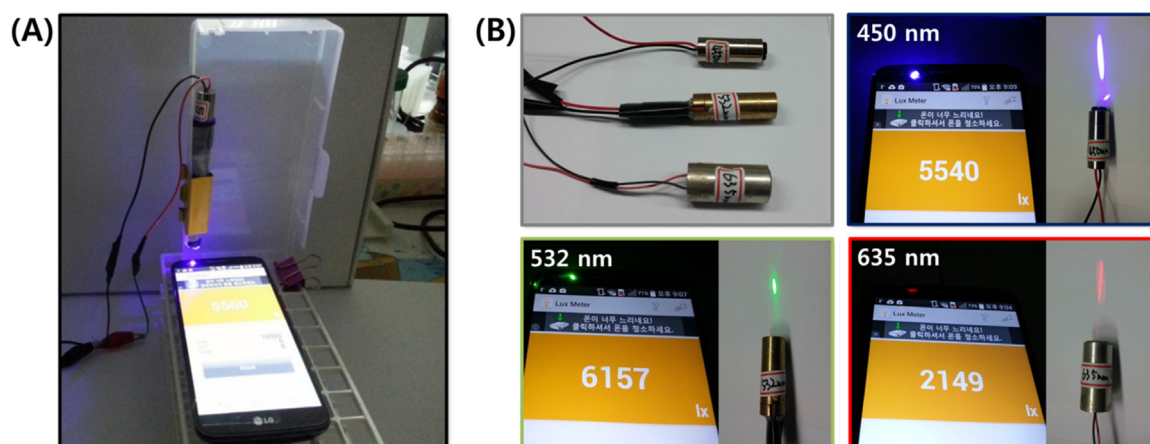


Fig. 2. Photographs of smartphone screens showing the reactivity of the smartphone-embedded illumination sensor to different light spectra. (A) Laser diode fixed above the sensor using plastic scaffolding. (B) Red (635 nm), green (532 nm), and blue (450 nm) lasers applied to the illumination sensor. (For interpretation of the references to color in this figure legend, the reader is referred to the web version of this article.)

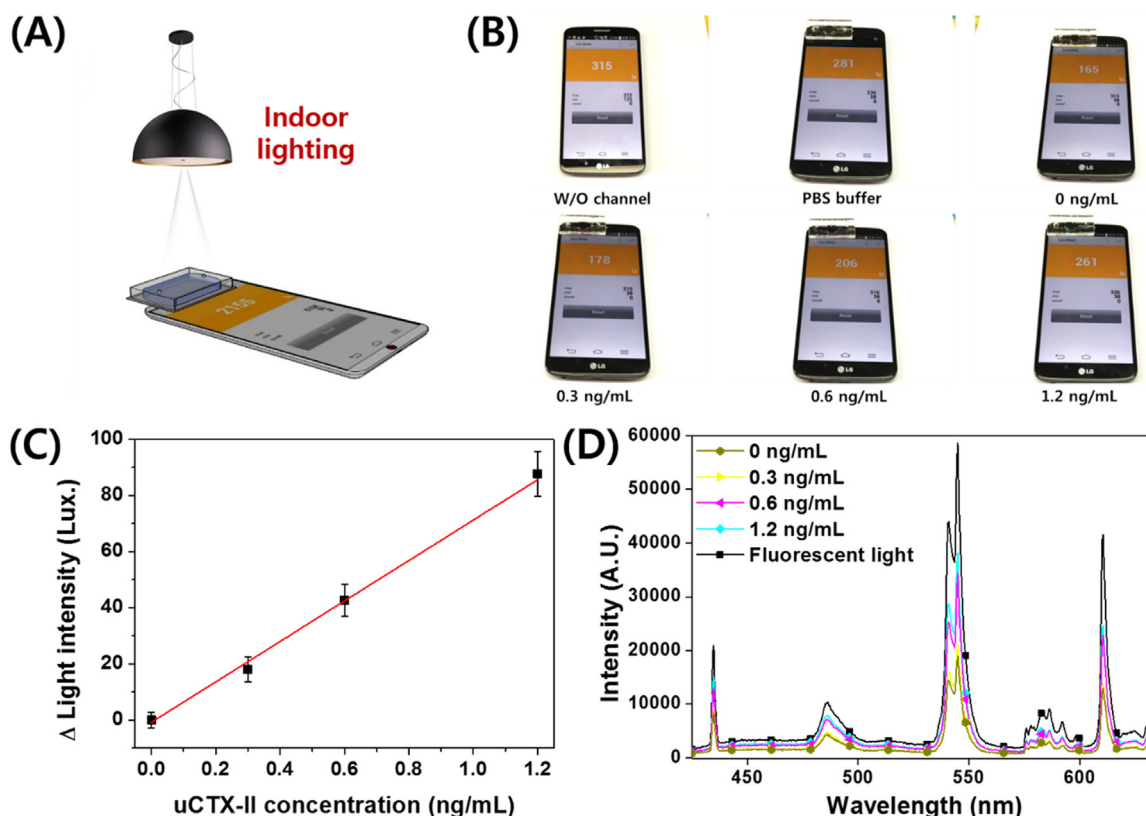


Fig. 3. (A) Schematic illustration of the indoor lighting-based biosensing platform. (B) Screen images obtained from the illumination sensor for uCTX-II concentration ranging from 0 to 1.2 ng/mL. (C) Calibration curve constructed for the uCTX-II assay based on indoor lighting. Each data point represents the average and standard deviation of independent triplicate tests. (D) Corresponding spectral intensity of the uCTX-II sample obtained using a spectrophotometer.

assay, interfered with the penetration of the fluorescent light. Therefore, the light intensity decreased with increasing target concentration. To confirm the reproducibility of the assay, tests were conducted in triplicate using the same uCTX-II sample under the same pH, temperature, and reaction time condition. The calculated coefficient of variation (COV) and R^2 value was approximately 10% and 0.98, indicating that the assay was reproducible. These reliable assay results verify that fluorescent light can be used as a light source for our biosensing system.

To confirm the correlation between the changes in fluorescent light intensity and the precipitation reaction as a function of the immunoblot-based uCTX-II assay, spectral variations in the intensity of the fluorescent light that passed through the biosensing channel were analyzed using a modular spectrometer. The intensity changed in proportion to the increase in uCTX-II concentration [Fig. 3(D)], indicating that the insoluble precipitate interfered with the penetration of the indoor light in the biosensing channel. The precipitate blocked not only a specific wavelength but also the entire spectrum of the indoor lighting. Thus, the lux value measured by the smartphone-embedded illumination sensor reflects the integrated light intensity of the entire light source spectrum. The two assays conducted using the illumination sensor with the spectrometer verified that the lux value of the intensity from the illumination sensor is that for the entire light source. In addition, the immunoblot-based illumination sensor demonstrated a relatively high optical signal in comparison with that of a typical optical analysis used in a monochromatic system. We showed that uCTX-II can be analyzed quantitatively with the illumination sensor and indoor lighting. In addition, with our biosensing system, biomarkers with a specific antibody pair can be measured without a target-specific light source, whereas the conventional optical instrument requires an additional device for

use as the target-focused light source. Therefore, our biosensing platform is a practical POCT device for disease diagnosis.

3.3. uCTX-II analysis using sunlight

As natural ambient light, sunlight is a useful energy source with a wide wavelength spectrum of high intensity. Because the entire wavelength range of a light source interferes with the immunoblot-based precipitation assay, sunlight can be a valuable light source for our optical sensing system, and a sunlight-based illumination sensor can be implemented without additional equipment. To confirm the reactivity of the illumination sensor to sunlight, the intensity of direct sunlight was measured using the lux meter application. The smartphone-embedded illumination sensor registered a lux value of 10,000 lx, which is the maximum lux intensity that the sensor can measure. Then, the dopamine-coated biosensing channel with PBS solution was applied to the sensor and the maximum intensity of the direct sunlight was measured as 7000 lx. We then analyzed the uCTX-II using sunlight. Fig. 4(A) shows the biosensing channel containing the precipitate from the uCTX-II assay located on the illumination sensor of the smartphone at which the change in light intensity was registered. The lux value changed in accordance with the concentration of the applied uCTX-II [Fig. 4(B)]. This result clearly shows that uCTX-II can be reliably assessed using natural light and without an artificial light source.

We conducted the same assay to evaluate uCTX-II in the shade [Fig. 4(C)]. First, we measured the light intensity in the shade as 5000 lx and then measured the light intensity with the dopamine-coated biosensing channel with PBS buffer in place as 3000 lx. Finally, uCTX-II was measured under the same conditions as the previous assay but in the shade. Fig. 4(D) presents the calibration

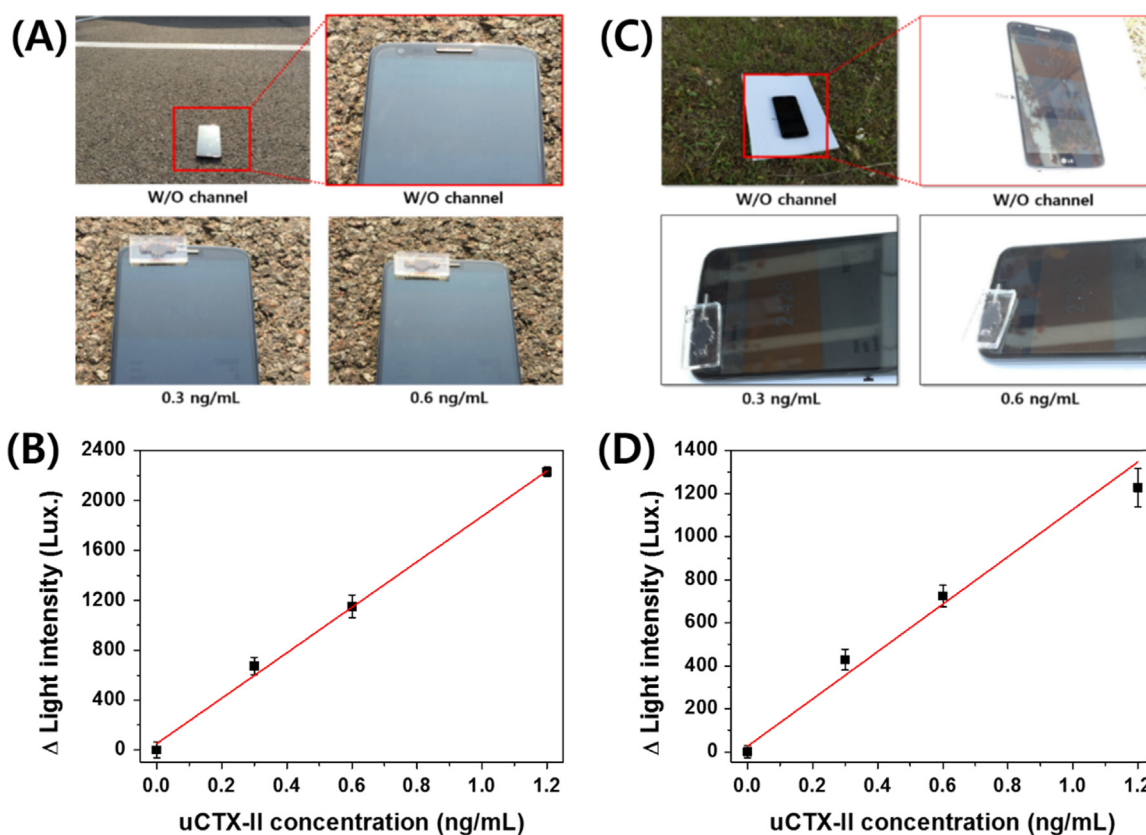


Fig. 4. (A) Photographs of the direct sunlight-based illumination sensor with uCTX-II concentrations of 0, 0.3, 0.6 and 1.2 ng/mL. (B) Calibration curve for the uCTX-II competition assay for direct sunlight. The mean of independent triplicate analyses is shown, and error bars indicate standard deviations. (C) Same as (A) but for shade condition. (D) Calibration curve for the uCTX-II competition assay for shade condition.

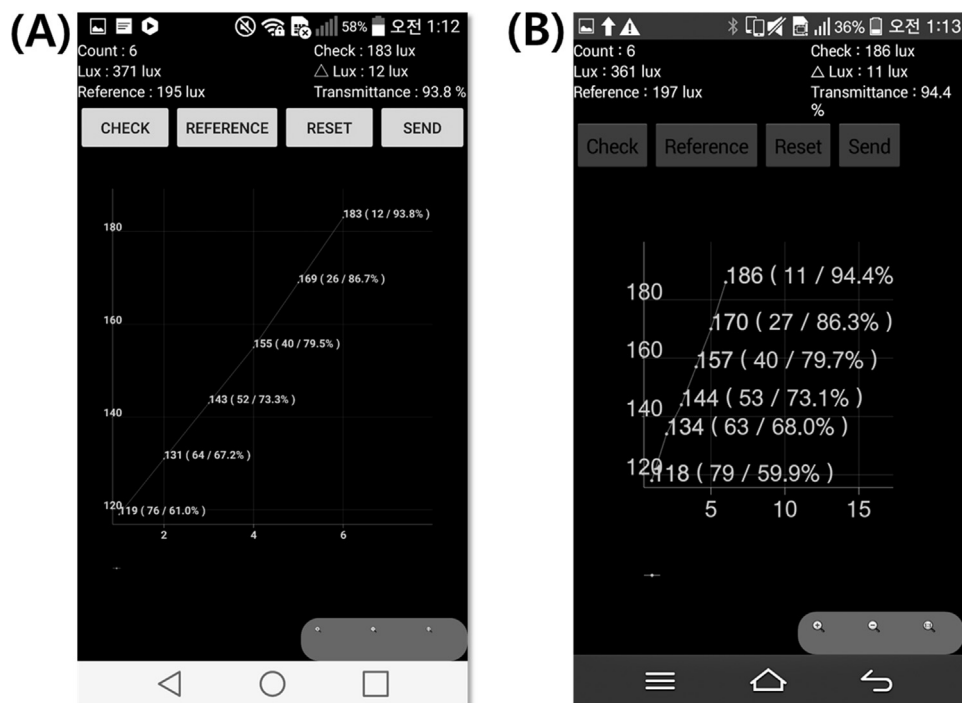


Fig. 5. Screen shots of the AjouLuxMeter application for an Android smartphone showing the information, functions, calibration curve. (A) LG G3 smartphone display after the assay of uCTX-II in the concentration range of 0–5 ng/mL under indoor lighting. (B) Vega Iron smartphone display of the same assay as in (A) and under indoor lighting.

Table 1

Transmittance found with the LG G3 smartphone-based biosensing system for different concentrations of uCTX-II (ng/mL) under different light conditions.

Light source	uCTX-II concentration					
	0.0 ng/mL	0.3 ng/mL	0.6 ng/mL	1.2 ng/mL	2.5 ng/mL	5.0 ng/mL
Indoor lighting	60 ± 4%	66 ± 3%	71 ± 3%	78 ± 3%	86 ± 4%	92 ± 3%
Direct sunlight	60 ± 3%	66 ± 5%	72 ± 3%	80 ± 2%	84 ± 3%	91 ± 4%
Shade	59 ± 4%	67 ± 3%	72 ± 3%	79 ± 5%	85 ± 3%	92 ± 4%

curve for the uCTX-II assay in the shade, demonstrating the linear increase in intensity with uCTX-II concentration. To verify the reproducibility of the biosensing platform using indoor and outdoor lights, the same uCTX-II assay was conducted under same condition at least three times. The calculated COV values were 10%, 7%, and 8% ($R^2=0.98, 0.97$, and 0.97) for each test in which fluorescent light, direct sunlight, and shade condition were used, which indicates that our biosensing platform possesses high reproducibility and accuracy. Although the different light sources have diverse spectra, including single, multiple, or whole wavelengths, reliable test results were obtained, indicating that the illumination sensor-based biosensing platform can be used in any lighting environment.

3.4. Mobile application for the smartphone-based optical sensor

In the test discussed in the preceding subsection, uCTX-II was successfully analyzed with the use of diverse light sources, while the lux value scale for the entire uCTX-II assay depended on the type of light source used. Therefore, there must be a standard set for the acquired signal to improve the applicability of the sensing system. Thus, we developed an Android-based application named “AjouLuxMeter”. Fig. 5 shows two screens of information and calibration curves obtained by AjouLuxMeter along with the various functions available.

Information at the top of the screen includes the assay number (“Count”), current lux (“Lux”), reference lux (“Reference”), registered lux (“Check”), the difference between the reference lux and the registered lux (“ Δ Lux”), and the ratio of reference lux to registered lux (“Transmittance”). In the middle of the screen, the “CHECK” button is for registration of the current lux, the “REFERENCE” button is for registration of the reference lux, “RESET” deletes all information on the screen, and “SEND” sends the acquired lux value to an e-mail address. The bottom of the screen shows the calibration curve, with information on the lux based on the assay results.

To establish the standard for intensity for each light source, the dopamine-coated biosensing channel containing PBS buffer was used as a reference channel. The lux value from each light source was registered as a reference value. Next, the change in light intensity from each assayed uCTX-II test set was analyzed by calculating the differences between the reference values and each test result. In addition, each result value was divided by the reference value to calculate the transmittance. Using the AjouLuxMeter software, the uCTX-II assay was conducted under the same conditions as the previous test, with fluorescent light as the first light source.

To verify that the illumination sensor platform can be used on different smartphones, we compared the performance of the LG G3 and the Vega Iron (IM-A870K) smartphones. Under indoor lighting conditions, both phones registered ~ 365 lx, indicating that the reactivity of the illumination sensor on each smartphone was similar. From this, we assumed that the smartphone-embedded sensor would demonstrate the same ability to respond to ambient light, thus allowing the implementation of our biosensing platform in different Android smartphones under the same

conditions. On the basis of the light intensity results, we evaluated the response of the phones to a uCTX-II concentration range of 0–5 ng/mL. For the 0 ng/mL uCTX-II assay, the smartphones registered 119 (G3) and 118 (Nexus) lx (Fig. 5), which again shows that the reactivity of both smartphones to the same light source was similar. The lux value obtained by the G3 smartphone in the uCTX-II assay changed proportionally according to the uCTX-II concentration, and the 33% transmittance completely changed over the entire uCTX-II assay [Fig. 5(A)]. The result of the uCTX-II assay on the Iron smartphone was similar, with the lux value gradually changing with the applied uCTX-II samples, and the approximately 34% transmittance changed under same test conditions as for the G3 [Fig. 5(B)]. Based on the obtained results, the limit of detection (LOD) from the G3 and Iron, which was calculated as 3.3 times the standard deviation of the background signal divided by the slope of the calibration curve, was 0.25 and 0.20 ng/mL. To confirm the reproducibility of each smartphone-based uCTX-II assay, the same uCTX-II samples were repetitively tested under same condition including the temperature, pH and reaction time. The coefficient of variation and the R^2 value for uCTX-II assay was found to be approximately 5% and 0.98, indicating the high stability of the developed biosensing method for the uCTX-II assay. These results show that our illumination sensor can be used with smartphones from different manufacturers, and that the uCTX-II level can be accurately measured.

3.5. Ambient light-based uCTX-II evaluation using AjouLuxMeter

To verify that the AjouLuxMeter software is applicable for different ambient light sources, we used the G3 smartphone to compare sunlight- and indoor lighting-based uCTX-II assays. uCTX-II in the concentration range of 0–5 ng/mL was assayed under same conditions used in the previous test with indoor lighting, direct sunlight, and shade. The data in Table 1 show that the transmittance increased proportionally with the increase in uCTX-II concentration for each light source.

The changes in the transmittance over the entire uCTX-II assay range for indoor lighting, direct sunlight, and shade were 32%, 31%, and 33%, respectively, which shows that the light intensity was altered at a certain ratio based on the immunoblotting assay. Thus, the transmittance-based optical sensing platform seems feasible. To confirm the similarity of test results for the different light sources, the variability of the calculated transmittance for each uCTX-II concentration was approximately 5%. Therefore, uCTX-II can be accurately assessed under any ambient light condition without the need for an additional device for a light source. The COV and R^2 for the uCTX-II assay based on the triply repeated test result under same condition were found to be 5% and 0.97, indicating the suitability of the ambient light-based illumination sensor for use in the diagnosis of OA. The LODs from the direct sunlight and shade-based assay were 0.2 and 0.19 ng/mL, respectively. The similar LOD values from the various light sources with different type of smartphone were obtained as approximately 0.2 ng/mL. In the healthy human, the uCTX-II level is commonly below 1 ng/mL, which is employed as a cut-off value for the evaluation of OA. Considering the cut-off value, the developed

biosensing method could distinguish the uCTX-II level in healthy human vs. OA patients. Also, because the registered dynamic range of uCTX-II covers the clinical demand for OA diagnosis (Garnero et al., 2002, 2003), the uCTX-II levels could be reliably assessed on the developed device. Based on the result, we show that a practical smartphone-based POCT device can provide simple quantification and is easy to operate. It has the potential to be a promising tool for accurate clinical diagnosis.

4. Conclusions

This study demonstrated a novel optical biosensor based on a smartphone-embedded illumination sensor. By integrating the immunoblotting-based biosensor with the smartphone, an immediate and accurate analysis of the analyte uCTX-II was possible without the use of professional equipment and special software under various ambient light conditions. Moreover, the entire biosensing system is embedded and uses the built-in capabilities of the smartphone. A notable advantage of this biosensing system is that it is simple to operate, thus allowing its use by untrained and non-medical profession personnel. Based on the reliable results of this study, the biosensing system presented here has the potential to be a POCT device for OA diagnosis.

Acknowledgment

This work was supported by the National Research Foundation (NRF-2016R1A2B4006564) of Korea and the Priority Research Centers Program (2009-0093826).

References

- Bandodkar, A.J., Wang, J., 2014. Trends Biotechnol. 32, 363–371.
- Breslauer, D.N., Maamari, R.N., Switz, N.A., Lam, W.A., Fletcher, D.A., 2009. PLoS One 4, e6320.
- Chun, H.J., Park, Y.M., Han, Y.D., Jang, Y.H., Yoon, H.C., 2014. Biochip J. 8, 218–226.
- Elsaid, K.A., Chichester, C.O., 2006. Clin. Chim. Acta 365, 68–77.
- Eyre, E.R., Weis, M.A., Wu, J.-J., 2008. Methods 45, 65–74.
- Garnero, P., Ayral, X., Rousseau, J.C., Christgau, S., Sandell, L.J., Dougados, M., Delmas, P.D., 2002. Arthritis Rheum. 46, 2613–2624.
- Garnero, P., Conrozier, T., Christgau, S., Mathieu, P., Delmas, P.D., Vignon, E., 2003. Ann. Rheum. Dis. 62, 939–943.
- Garnero, P., Peterfy, C., Zaim, S., Schoenharthart, M., 2005. Arthritis Rheum. 52, 2822–2829.
- Han, Y.D., Chun, H.J., Yoon, H.C., 2014. Biosens. Bioelectron. 29, 259–268.
- Kong, S.Y., Stabler, T.V., Criscione, L.G., Elliott, A.L., Jordan, J.M., Kraus, V.B., 2006. Arthritis Rheum. 54, 2496–2504.
- Lee, H., Dellatore, S.M., Miller, W.M., Messersmith, P.B., 2007. Science 318, 426–430.
- Mabey, D., Peeling, R.W., Ustianowski, A., Perkins, M.D., 2004. Nat. Rev. Microbiol. 2, 231–240.
- Martinez, A.M., Phillips, S.T., Carrilho, E., Thomas, S.W., Sindi, H., Whitesides, G.M., 2008. Anal. Chem. 80, 3699–3707.
- O'Driscoll, S., MacCraith, B.D., Burke, C.S., 2013. Anal. Methods 5, 1904–1908.
- Pablos, J.L., Trigo-Lo'pez, M., Serna, F., Garc'ia, F.C., Garc'ia, J.M., 2014. Chem. Commun. 50, 2484–2487.
- Park, Y.M., Han, Y.D., Kim, K.R., Zhang, C., Yoon, H.C., 2015a. Anal. Methods 7, 6437–6442.
- Park, Y.M., Kim, S.J., Lee, K.J., Yang, S.S., Min, B.-H., Yoon, H.C., 2015b. Biosens. Bioelectron. 67, 192–199.
- Peeling, R.W., Mabey, D., 2010. Clin. Microbiol. Infect. 16, 1062–1069.
- Reijman, M., Hazes, J.M., Bierma-Zeestra, S.M., Koes, B.W., Christgau, S., Christiansen, C., Uitterlinder, A.G., Pols, H.A., 2004. Arthritis Rheum. 50, 2471–2478.
- Roda, A., Michelini, E., Cevenini, L., Calabria, D., Calabretta, M.M., Simoni, P., 2014. Anal. Chem. 86, 7299–7304.
- Salles, M.O., Meloni, G.N., de Araujo, W.R., Paixão, T.R.L.C., 2014. Anal. Methods 6, 2047–2052.
- Uys, P.W., Warren, R., van Helden, P.D., 2009. J. Clin. Microbiol. 47, 1484–1490.